HHS Public Access

Author manuscript

*J Physiol*. Author manuscript; available in PMC 2021 May 01.

Published in final edited form as:

*J Physiol*. 2020 May ; 598(9): 1775–1790. doi:10.1113/JP278327.

# Diurnal properties of voltage-gated $Ca^{2+}$ currents in suprachiasmatic nucleus and roles in action potential firing

**Beth A. McNally**, **Amber E. Plante**, **Andrea L. Meredith***

Dept. of Physiology, University of Maryland School of Medicine, Baltimore, MD, 21201

## Abstract

The mammalian circadian clock encodes time via rhythmic action potential activity in the suprachiasmatic nucleus (SCN) of the hypothalamus, which governs daily rhythms in physiology and behavior. SCN neurons exhibit 24-hr oscillations in spontaneous firing, with higher firing during day compared to night. Several ionic currents have been identified that regulate SCN firing, including voltage-gated $Ca^{2+}$ currents, but the circadian regulation of distinct voltage-gated $Ca^{2+}$ channel (VGCC) components has not been comprehensively addressed. In this study, whole-cell L- (Nimodipine-sensitive), N- and P/Q- (ω-agatoxin IVA, ω-conotoxin GVIA, ω-conotoxin MVIIC-sensitive), R- ($Ni^{2+}$-sensitive), and T-type (TTAP2-sensitive) currents were recorded from day and night SCN slices. Using standard voltage protocols, $Ni^{2+}$-sensitive currents comprised the largest proportion of total VGCC current, followed by Nimodipine-, AgaIVA-, ConoGVIA-, and TTAP2-sensitive currents. Only the Nimodipine-sensitive current exhibited a diurnal difference in magnitude, with daytime current larger than night. No diurnal variation was observed for the other $Ca^{2+}$ current subtypes. The difference in Nimodipine-sensitive current was due to larger peak current activated during the day, not differences in inactivation, and was eliminated by Bay K. Blocking L-type channels decreased firing selectively during the day, consistent with higher current magnitudes, and reduced SCN circuit rhythmicity recorded by multielectrode arrays. Yet blocking N-, P/Q-, and R-type channels also decreased daytime firing, with little effect at night, and decreased circuit rhythmicity. These data identify a unique diurnal regulation of L-type current among the major VGCC subtypes in SCN neurons, but also reveal that diurnal modulation is not required for time-of-day specific effects on firing and circuit rhythmicity.

### Keywords

voltage-gated $Ca^{2+}$ channel; $Ca^{2+}$ currents; action potential; intrinsic excitability; circadian rhythm; suprachiasmatic nucleus

*Corresponding author: Andrea L. Meredith, Dept. of Physiology, University of Maryland School of Medicine, 655 W. Baltimore St., Baltimore, MD 21201, Tel: (410) 706-5991, Fax: (410) 706-8341, ameredith@som.umaryland.edu.

AUTHOR CONTRIBUTIONS

All experiments were performed in the lab of Andrea Meredith in the Dept. of Physiology at the University of Maryland School of Medicine. B.A.M., A.E.P., and A.L.M. designed the experiments and analyzed the data. B.A.M. and A.E.P. performed the experiments. A.L.M. wrote the manuscript. All authors approved the final version of the manuscript.

DISCLOSURES/COMPETING INTERESTS

The authors declare that they have no competing interests.

## INTRODUCTION

Mammalian circadian rhythms in physiological functions and behaviors are governed by a central clock comprised of a network of spontaneously active neurons located within the hypothalamic suprachiasmatic nucleus (SCN) (Moore & Eichler, 1972; Stephan & Zucker, 1972; Lehman et al., 1987). SCN neurons generate a time signal by producing 24-hr oscillations in action potential firing, characterized by relatively higher firing frequency during the day (6-10 Hz) compared to the night (0-5 Hz)(Yamazaki et al., 1998; Pennartz et al., 2002; Kuhlman & McMahon, 2006). These circadian rhythms in action potential firing are driven by the coordinated activity of ion channels that control the intrinsic excitability of SCN neurons between day and night (de Jeu et al., 1998; Pennartz et al., 2002; Jackson et al., 2004; Nitabach et al., 2005; Kuhlman & McMahon, 2006; Meredith et al., 2006). The ionic currents involved in action potential firing include voltage-gated $Na^+$ currents (Flourakis & Allada, 2015), voltage-gated $K^+$ currents (Itri et al., 2005; Itri et al., 2010; Hermanstyne et al., 2017), $Ca^{2+}$-activated $K^+$ currents (Cloues & Sather, 2003; Meredith et al., 2006; Whitt et al., 2016), and $Ca^{2+}$ currents (Pennartz et al., 2002; Cloues & Sather, 2003; Jackson et al., 2004).

The major $Ca^{2+}$ channels expressed in the SCN include voltage-gated $Ca^{2+}$ channel (VGCC) subtypes including L-type $Ca^{2+}$ channels, P/Q-type $Ca^{2+}$ channels, N-type $Ca^{2+}$ channels, R-type $Ca^{2+}$ channels, and T-type $Ca^{2+}$ channels (Pennartz et al., 2002; Cloues & Sather, 2003; Kim et al., 2005; Nahm et al., 2005), as well as intracellular inositol trisphosphate receptors ($IP_3Rs$)(Hamada et al., 1999) and ryanodine receptors (RyRs)(Diaz-Munoz et al., 1999; Pfeffer et al., 2009). Of these, the L-type $Ca^{2+}$ current has been shown exhibit circadian regulation in SCN neurons, with larger currents during the day compared to night (Pennartz et al., 2002). L-type currents also mediate oscillations in subthreshold membrane potential and contribute to the activation of $Ca^{2+}$-activated $K^+$ currents in SCN neurons during the day (Pennartz et al., 2002; Jackson et al., 2004; Whitt et al., 2018). Consistent with this, selective inhibition of LTCC currents reduces the firing rate of SCN neurons during the day but has little effect at night (Pennartz et al., 2002; Whitt et al., 2018). While these data support the hypothesis that L-type $Ca^{2+}$ channels play an important role in SCN excitability by contributing to daytime firing rate, L-type currents comprise only ~30% of the total $Ca^{2+}$ current during the day and ~18% of the total $Ca^{2+}$ current at night (Whitt et al., 2018), leaving open the amount that other VGCC currents may differentially contribute to $Ca^{2+}$ current and firing rate during the day and night SCNs.

Furthermore, the role of intracellular $Ca^{2+}$ channels in action potential rhythmicity is also not well-understood. Although RyRs were originally suggested to contribute to circadian rhythms in cytosolic $Ca^{2+}$ (Ikeda et al., 2003), several studies show RyRs also regulate action potential firing both during the day and at night. RyR inhibition caused a decrease in firing rate in the majority of SCN neurons recorded during the day and night (Ikeda et al., 2003; Aguilar-Roblero et al., 2007; Aguilar-Roblero et al., 2016). However, the effects of RyR inhibitors on firing frequency can be heterogeneous between individual neurons (Diaz-Munoz et al., 1999). Activating RyRs can also significantly reduce action potential frequency during the day (Whitt et al., 2018) and the night (Aguilar-Roblero et al., 2016). Consistent with this, in some SCN neurons RyR inhibition caused a significant increase in

firing rate during the night, via loss of activation of the BK $Ca^{2+}$-activated $K^+$ current (Whitt et al., 2018). Since RyRs can influence firing rates in a heterogeneous manner, it is important to understand the role of these and other intracellular $Ca^{2+}$ channels in circuit level firing activity and rhythmicity.

The goal of this study was to understand whether there exists systematic circadian regulation of $Ca^{2+}$ current, and how this may regulate action potential rhythmicity in SCN. To address this, we comprehensively assessed the circadian regulation of each of the major $Ca^{2+}$ current subtypes under equivalent whole-cell recording conditions from acute SCN brain slices prepared during the day or during the night. The effects of pharmacological inhibition of VGCCs and intracellular $Ca^{2+}$ channels were evaluated on both short-term multi-unit action potential activity and long-term rhythmicity using acute and cultured SCN slices, respectively. The results link observations at the membrane (macroscopic current levels), neuron (action potential firing), and circuit (rhythmicity), to establish the basic roles for each of the major $Ca^{2+}$ current subtypes in SCN output.

## METHODS

### Ethical Approval and Animals

WT male and female C57BL/6J were used at 3–6 wk old (acute SCN slice experiments) or Postnatal day 4-5 (organotypic SCN cultures). Animals were housed on a standard 12:12-h light–dark cycle (for day timepoint harvests) or a reverse 12:12-h light–dark cycle (night). All procedures involving mice were conducted in accordance with the University of Maryland School of Medicine Animal Care and Use Guidelines and approved by the Institutional Animal Care and Use Committee (Protocol #1217011) Animals had access to food and water ad libitum. Animals were humanely killed by inhalation of saturating isoflurane vapor to sedation, followed by decapitation and exsanguination. The experiments in this study conform to the guidelines for the use of animals presented in Grundy (2015).

### Acute SCN slice preparation and electrophysiology

Mice were sacrificed 1-3 hrs after lights on (zeitgeber time, ZT1-3) for day recording timepoints or under red light illumination 2-4 hrs after lights off (ZT14-16) for night recording timepoints, as described previously (Whitt et al., 2018). Brains were rapidly removed and placed in ice-cold sucrose-substituted saline containing (in mM): 1.2 $MgSO_4$, 26 $NaHCO_3$, 1.25 $Na_2HPO_4$, 3.5 KCl, 3.8 $MgCl_2$, 10 glucose and 200 sucrose. Coronal slices were cut at 300 μm on a VT1000S vibratome (Leica Microsystems, Wetzlar, Germany) at 3–4 °C. Slices containing SCN were recovered for 1-3 h at 25 °C submerged in oxygenated artificial cerebrospinal fluid (ACSF) (in mM: 125 NaCl, 1.2 $MgSO_4$, 26 $NaHCO_3$, 1.25 $Na_2HPO_4$, 3.5 KCl, 2.5 $CaCl_2$ and 10 glucose (300-305 mOsM). Slices containing SCN were transferred to the recording chamber (RC26GLP/PM-1; Warner Instruments, Hamden, CT, USA) with gravity flow bath perfusion of 1-2 ml $min^{-1}$ oxygenated ACSF at 25 °C. Neurons were visualized with a Luca-R DL-604 EMCCD camera (Andor, Belfast, UK) under IR-DIC illumination on an FN1 upright microscope (Nikon, Melville, NY, USA). Recordings were made from cells in the center of the SCN, with cell capacitances ranging from 5-11 pF. Recording windows were at the peak (ZT4-8)

and nadir (ZT17-21) of the circadian rhythm in spontaneous action potential firing, corresponding to the ‘day’ and ‘night’ time points, respectively.

Whole-cell current- and voltage-clamp recordings were made with a MultiClamp 700B amplifier, 1440 Digidata and pCLAMP v10.3 software (Molecular Devices, Sunnyvale, CA, USA). Data were acquired at a 50 or 100 kHz sampling rate for voltage and current clamp mode, respectively, and online filtered at 10 kHz. A standard P/4 leak subtract protocol was used for whole-cell voltage-clamp recordings. Drugs were focally perfused to the bath at a flow rate of 1 mL $min^{-1}$ via gravity flow at the final concentrations indicated.

$Ca^{2+}$ currents were recorded in whole-cell voltage-clamp mode using borosilicate glass electrodes (4-7 MΩ, Sutter Instruments, Novato, CA, USA) filled with internal solution of (in mM): 115 Cs-methanesulfonate, 10 tetraethylammonium chloride (TEA-Cl), 10 HEPES, 0.5 EGTA, 2 $MgCl_2$, 20 sodium phosphocreatine, 2 $Na_2ATP$, and 0.3 $Na_3GTP$, pH 7.3 (~280 mOsM). The bath ACSF was (in mM): 68 NaCl, 3.5 KCl, 1 $NaH_2PO_4$, 26.2 $NaHCO_3$, 1.3 $MgSO_4$, 2.5 $CaCl_2$, 10 glucose, 60 TEA-Cl, and 3 CsCl (pH 7.4) (~300 mOsM). Total voltage-activated inward currents were recorded in 1 μM tetrodotoxin before and during focal perfusion of $Ca^{2+}$ channel inhibitors. Post-inhibitor currents were recorded 4 mins after drug wash-on. A 10-15-minute wash-out was applied between cells. For the standard voltage step protocol, currents were elicited from a holding potential of −90 mV, stepping from −100 to 50 mV for 150 ms in 10-mV increments. Action potential commands were delivered from a holding potential of −150 mV to remove inactivation. The day waveform stepped to the inter-spike potential (−48 mV) with a sequence of three action potentials (Peak, 8 mV; $t_{½}$, 10 ms; and afterhyperpolarization (AHP)/antipeak, −54 mV). The night action potential command stepped to inter-spike potential (−51 mV) with a sequence of three action potentials (Peak, 0.9 mV; $t_{½}$, 3.9 ms; and AHP/antipeak, −57 mV). Calcium current subtypes were isolated by subtracting currents in the presence of respective $Ca^{2+}$ channel inhibitors from baseline (total $Ca^{2+}$) currents prior to drug application. Three current responses were averaged per cell and normalized to cell capacitance. Voltage values were adjusted for the liquid junction potential (9 mV). $R_a$ was <25 MΩ with less than ±5% change (on average ~15 MΩ). $R_s$ was compensated at 60%.

## Action Potential Recordings and Calcium Oscillations

In whole-cell current-clamp mode, calcium-dependent membrane potential oscillations were recorded in chronic bath TTX (1 μM) application with pipette solution (in mM): 123 K-methanesulfonate, 9 NaCl, 0.9 EGTA, 9 HEPES, 14 Tris-phosphocreatine, 2 $Mg^{2+}$-ATP, 0.3 Tris-GTP, and 2 $Na^{2+}$-ATP with osmolality of ~310 mOsM, and pH adjusted to 7.3 with KOH) and ACSF bath solution (in mM): 125 NaCl, 26 $NaHCO_3$, 10 glucose, 3.5 KCl, 2.5 $CaCl_2$, 1.25 $Na_2HPO_4$, and 1.2 $MgSO_4$ with osmolality adjusted to ~300 mOsM with glucose). Nimodipine (10 μM) was applied chronically to the bath as indicated. Data were acquired in current-clamp mode in 10-s sweeps at the cell’s resting membrane potential (spontaneous oscillations) and at a series of holding voltages from −60mV to 0 mV, in 10 mV increments (voltage-dependent oscillations). Membrane potential oscillations were defined as >5 mV change in membrane potential (peak to trough) at a frequency of >0.2 Hz. Representative traces were filtered at 2 kHz.

Extracellular action potentials were recorded as multi-unit activity in current clamp mode with electrodes (10-40 MΩ) filled with 2 M NaCl. Action potentials were recorded for 0.5 to 1-minute sweeps at a sampling rate of 50 kHz and filtered at 1 kHz. Firing frequency was determined by threshold-based templates using Clampfit v10.3 software (Molecular Devices, Sunnyvale, CA, USA), setting the threshold >50% above the noise. Baseline action potential frequencies were recorded in ACSF alone, and $Ca^{2+}$ channel inhibitors were bath-applied individually by gravity perfusion.

## Organotypic SCN culture and MEA Recordings

Coronal sections (300 μm) were prepared from P4-5 brains with a manual tissue slicer (Stoelting, Wood Dale, IL, USA) in ice-cold dissection media: Bicarbonate-free DMEM (Gibco; 12100-046), 10 mM HEPES (pH 7.2), 100 U/mL Penicillin/Streptomycin (Mediatech, Manassas, VA, USA; 30-002-CI), 2 mM L-glutamine (Mediatech, Manassas, VA, USA; 25-005-CI). Slices containing the rostro-caudal center of the SCN were plated directly onto multi-electrode array (MEA) probes (Alpha MED Scientific Inc., Osaka, Japan; MED-P210A), prepared with 0.01% polyethyleneimine (PEI;Sigma, Darmstadt, Germany;P3143) as per the manufacturer's instructions (MEA preparations (2017), available at http://www.med64.com/documentation/) and pre-coated with 500 μL of 0.1 mg/mL collagen from calf-skin overnight (Sigma, Darmstadt, Germany;C8919) as described (Montgomery et al., 2013; Whitt et al., 2016).Organotypic SCNs were cultured as interface explants in 300 μL of culture media in a 5% $CO_2$ incubator at 37°C as described (Montgomery et al., 2013; Whitt et al., 2016). Culture media contained: 50% MEM (Gibco, Gaithersburg, MD, USA; 11095-080), 25 mM HEPES (pH 7.2), supplemented with 25% horse serum (Gibco, Gaithersburg, MD, USA; 16050-130), 100 mg glucose, 100 U/mL Penicillin/Streptomycin (Mediatech, Manassas, VA, USA; 30-002-CI), and 2 mM L-glutamine (Mediatech, Manassas, VA, USA; 25-005-CI). Media was changed every 48 hours for the first 8 days in culture, and every 72 hours thereafter (50% volume exchange). 20 μM cytosine β-D-arabinofuranoside (Ara-C, Sigma, Darmstadt, Germany; C6645) was added to the culture media on day 2 to inhibit glial cell growth. Extracellular action potential recordings were performed at days 10-24 in culture using a MED64-Plex8 system (Alpha MED Scientific Inc., Osaka, Japan). Spontaneous action potential activity was acquired from 5 sec sweeps every 5 minutes, for 3 days of baseline and 3 days after drug application. Data were acquired with low cut frequency 100 Hz and high cut frequency 10000 Hz (Mobius vWin7, Alpha MED Scientific Inc., Osaka, Japan), and firing frequency was determined from each 5 second sweep using a threshold-based counting at ~1.5X the level of baseline noise (typically between −10 to −25 μV). Drugs or vehicle controls were added to the culture media along with a 50% media exchange applied during the middle of the third trough in baseline activity (identified based on the timing of the second trough in baseline activity). Drugs were diluted to 2X the working concentration in culture media, pre-warmed in a 5% $CO_2$ incubator at 37°C, and was then used for a 50% media exchange to achieve a final working concentration of 1X.

## Drugs

Drugs were used at final concentrations of 1 μM tetrodotoxin (TTX; Alomone Labs, Jerusalem, Israel; T-550), 10 μM Nimodipine (Alomone Labs, Jerusalem, Israel; N150), 10

μM dantrolene (Dan; Sigma, Darmstadt, Germany; D9175), 1 μM cyclopiazonic acid (CPA; Alomone Labs, Jerusalem, Israel; C-750), 3 μM ω-conotoxin GVIA (ConoGVIA; Alomone Labs, Jerusalem, Israel; C-300), 3 μM ω-conotoxin MVIIC (ConoMVIIC; Alomone Labs, Jerusalem, Israel; C-150), 200 nM ω-agatoxin IVA (AgaIVA;Alomone Labs, Jerusalem, Israel; STA-500), 1 μM TTA-P2, (TTAP2;Alomone Labs, Jerusalem, Israel; T-155), 200 μM $CdCl_2$ ($Cd^{2+}$; Sigma; 529575), 30 μM $NiCl_2$ ($Ni^{2+}$; Sigma; 22387), and 5 μM Bay K8644 (Bay K; Sigma, Darmstadt, Germany; B133). Stocks (1000X) were prepared in DMSO (Nim, Dan, CPA, TTAP2, Bay K) or water (TTX, ConoGVIA, ConoMVIIC, AgaIVA, $Ni^{2+}$, $Cd^{2+}$) and stored at −20°C.

## Data Analysis and Statistics

Data were not collected or analyzed blinded. For voltage-clamp experiments, current-voltage relationships were constructed from the peak of the macroscopic current at each voltage. Inactivation was measured by normalizing the steady-state current (at 150 ms) to the peak current value ($I_{steady\text{-}state}/I_{Peak}$). Action potential-evoked current was determined from the second of three action potential commands, from a 1 ms window at the peak of the waveform. For current-clamp recordings in acute slices, extracellular firing frequency was determined from 30 s sweeps.

In MEA experiments, recording electrodes located within the boundaries of the SCN were identified with bright field optics at 4X magnification. For circadian rhythm analysis, a 2-hour moving window average was applied to smooth the raw data and plotted as frequency versus time. Recordings within the SCN were determined to be rhythmic if there was one circadian peak per 24-hr cycle (across 3 cycles), with the average peak value being ≥3 Hz above the trough value. Recordings that failed these criteria were classified as arrhythmic. Only the slices exhibiting rhythmic activity from ≥70% of electrodes within the SCN during baseline recordings were used for experiments. Period was calculated as the time interval between the daily peaks in action potential activity. The $\chi^2$ amplitude was determined from periodograms plotted from 3 cycles of baseline data and 3 cycles of data after drug application (two peaks and 3 troughs for each segment; (ClockLab, Actimetrics, Wilmette, IL, USA). The circadian amplitude is reported as the highest $\chi^2$ periodogram peak value above the 99% confidence interval corresponding to the period length manually calculated for each slice in baseline and post-drug or vehicle control conditions. For each slice, the $\chi^2$ amplitude of the circuit was measured from all electrodes within the SCN (rhythmic and arrhythmic). The $\chi^2$ amplitude was also separately calculated from only the rhythmic recordings within the SCN.

All data are reported in figures as mean ± SEM. For voltage-clamp and action potential recordings, the number of neurons is reported in the figure legends and used to generate the statistical comparison. Data for each condition was derived from a minimum of two animals, with one SCN slice per animal. All datasets passed tests for normality. Statistical significance was determined at $P < 0.05$ by using the following tests in Prism v8.0 (Graphpad Software, San Diego, CA, USA): Welch's unpaired *t*-test was used for pairwise comparisons of day versus night values for each $Ca^{2+}$ current subtype at a single voltage (Fig. 2I, 3C, 4D and 6F), Fisher's exact test was used for categorical data (i.e., number of neurons exhibiting

spontaneous calcium oscillations for day versus night), and one-way ANOVA with Bonferroni post-hoc was used to compare control extracellular firing frequency to frequencies with $Ca^{2+}$ channel inhibitors (Fig. 7B and C).

Paired Student's *t*-tests were used to compare MEA rhythm parameters before and after $Ca^{2+}$ channel inhibitor application (Fig. 8G–I). Both the number of recordings and number of slices are reported in the figure legends. For MEA data, the number of n's for statistical comparison is the number of slices, where the value for each slice represents the average of the recordings obtained from each slice.

## RESULTS

### Analysis of day versus night voltage-gated $Ca^{2+}$ currents in SCN

To determine the magnitude and properties of voltage-gated $Ca^{2+}$ currents, voltage-clamp recordings were performed from acute SCN slices prepared from mouse brains during the day (ZT4-8) and night (ZT17-21). Cells from the central region of the SCN were recorded in whole-cell configuration in the presence of 1 μM TTX and 60 mM TEA to inhibit voltage-gated $Na^+$ and $K^+$ channels, with 2.5 mM extracellular $Ca^{2+}$ and 0.5 mM EGTA in the internal solution. Under these conditions, robust inward $Ca^{2+}$ currents are observed in response to depolarizing voltage steps greater than −60 mV (Fig. 1A and B). These inward currents had maximal amplitudes ranging from 170 to 670 pA and were blocked by 200 μM $Cd^{2+}$. The maximum total inward and $Cd^{2+}$-sensitive currents peaked at −10 to 0 mV, both during the day and at night, and showed a rapid activation and a relatively slow inactivation.

To broadly distinguish different $Ca^{2+}$ channel subtypes present in SCN neurons, selective antagonists were applied individually, and the drug-sensitive current was isolated for each cell. The antagonists were expected to block effectively all the current from each $Ca^{2+}$ channel subtype since these drugs were focally applied at 133–4500X the $IC_{50}$ values (Mintz et al., 1992; Boland et al., 1994; Marchetti et al., 1995; Randall & Tsien, 1995; McDonough et al., 1996; Tottene et al., 1996; Zamponi et al., 1996; Lewis et al., 2000; Cloues & Sather, 2003; Dreyfus et al., 2010). During the day, partial $Ca^{2+}$ current inhibition was obtained with individually applied 10 μM Nimodipine (an L-type $Ca^{2+}$ channel inhibitor), 3 μM ω-conotoxin MVIIC (ConoMVIIC, N/P/Q-type), 3 μM ω-conotoxin GVIA (ConoGVIA, N-type), 200 nM ω-agatoxin IVA (AgaIVA, P/Q-type), 30 μM $Ni^{2+}$ (R-type), and 1 μM TTA-P2 (TTAP2, T-type) (Fig. 1C). While Nimodipine, ConoMVIIC/GVIA, and AgaIVA are generally selective for the indicated $Ca^{2+}$ channel subclasses, $Ni^{2+}$ is a less selective inhibitor of R-type current. However, no significant current reduction was found with application SNX-482 (200 nM, n=3), which more selectively inhibits $Ca_V2.3$ R-type channels (Newcomb et al., 1998). The lack of SNX-482-sensitive $Ca^{2+}$ current is consistent with previous observations in daytime SCN neurons (Cloues & Sather, 2003). Low concentrations of $Ni^{2+}$ can inhibit a small portion of L-type current (Cav1.2)(Zamponi et al., 1996) and one T-type channel isoform (Cav3.2)(Lee et al., 1999), but SCN neurons do not appear to express the $Ni^{2+}$ sensitive T-type isoform (Talley et al., 1999). $Ni^{2+}$ (30 μM) is not expected to inhibit N- or P/Q-type currents. Mibefradil caused some inhibition of L-type current (500 nM, n=3), reducing the utility of this T-type inhibitor. TTAP2 was used as a selective inhibitor for T-type channels ($IC_{50}$ = 22 nM)(Dreyfus et al., 2010). Overall, the

reduction in current with each inhibitor suggests the presence of all the major subtypes of $Ca^{2+}$ currents in SCN neurons. The largest components of the daytime current were sensitive to $Ni^{2+}$ and ConoGVIA (Fig. 1B and C), ranging from 11-73% and 22-57% and of the total current across cells, respectively. This was followed by contributions of Nimodipine-sensitive (13-60% of the total daytime $Ca^{2+}$ current), and AgaIVA-sensitive (9-42%) (Fig. 1B and C) currents. In contrast, few cells exhibited a TTAP2-sensitive current (27%, n=22 cells recorded). These data show that high voltage activated R-, N-, and L-type channels comprise the largest components of the total $Ca^{2+}$ current during the day in all SCN neurons, while low voltage-activated T-type channels are not as ubiquitous.

At night, $Ca^{2+}$ currents were sensitive to the same antagonists. Similar to daytime cells, the largest component of the nighttime current was also sensitive to $Ni^{2+}$ (Fig. 1B and C), ranging from 27-73% of the total current across cells. This was followed by contributions the TTAP2-sensitive (23-47%), ConoGVIA-sensitive (11-39%), AgaIVA-sensitive (9-30%), and Nimodipine-sensitive (9-36%) currents. Even though the nighttime T-type current comprised a larger portion of the total $Ca^{2+}$ current compared to day, there were still limited numbers of cells exhibiting a TTAP2-sensitive current at night (18%, n=49)(Fig. 1B and C). Thus, at night, like during the day, R-type channels comprise the largest component of the total $Ca^{2+}$ current. Yet unlike daytime recordings, T-type current makes a slightly larger contribution than the other $Ca^{2+}$ current subtypes.

Taken together, these data demonstrate the presence of several different subtypes of $Ca^{2+}$ channels in SCN neurons. Except for TTAP2-sensitve current, antagonist-sensitive $Ca^{2+}$ currents were obtained readily from most neurons at either time of day, suggesting that L-, N-, P/Q-, and R-type currents are present in all SCN neurons. The proportion of the total $Ca^{2+}$ current sensitive to each antagonist differed across cells, suggesting significant heterogeneity in the channel subtypes underlying these currents. In addition to variation between cells, the relative contribution of each current subtype to the total cellular $Ca^{2+}$ current also varied between day and night.

## L-type currents are diurnally regulated in SCN

To address whether the average $Ca^{2+}$ current subtype contribution differed as a result of circadian regulation, the antagonist-sensitive current magnitudes were compared between day and night. Across a large number of cells, no gross diurnal difference in the peak inward current in the presence of TTX was observed (Fig. 2A, I). Isolation of the voltage-gated $Ca^{2+}$ current with $Cd^{2+}$ showed a slightly higher peak current density during the day, but this difference was not statistically significant (Fig. 2B and I). To further analyze whether any individual $Ca^{2+}$ channel subtype might exhibit a more robust diurnal difference, specific subclasses were investigated using the selective inhibitors. Similar to prior studies (Pennartz et al., 2002; Whitt et al., 2018), the Nimodipine-sensitive current was found to exhibit a significant day versus night difference in magnitude, with larger currents during the day (Fig. 2C and I). On average, the daytime Nimodipine-sensitive current was twice as large as the nighttime current ($-16 \pm 2$ pA/pF versus $-8 \pm 1$ pA/pF; P=0.002). Interestingly, the peak of the current-voltage relationship shifted between day (−10 mV) and night (0 mV). In contrast, no other $Ca^{2+}$ current subtypes displayed a measurable day versus night difference

in current magnitude, or between the peaks of the current-voltage relationships (Fig. *D-I*). Current levels were as follows for AgaIVA- (−9 ± 2 versus −7 ± 1 pA/pF), ConoGVIA- (−15 ± 2 versus −12 ± 2 pA/pF), $Ni^{2+}$- (−15 ± 2 versus −15 ± 2 pA/pF), or TTAP2-sensitive (−6 ± 2 versus −9 ± 2pA/pF) currents.

In addition to activation of the current, measured at the peak current level obtained from the beginning of the activating voltage step, inactivation of each $Ca^{2+}$ current subtype was also assessed. Inactivation was quantified as the ratio of the steady-state current at the end of the 150 ms voltage step to the initial peak current ($I_{SS}/I_{peak}$). Inactivation did not vary between day and night for the Nimodipine-sensitive current (Fig. 3A). Both the voltage-dependence of inactivation (Fig. 3B), as well as the inactivation at the peak of the current voltage relationship were similar (Fig. 3C, $I_{SS}/I_{peak}$: 0.45 ± 0.03 versus 0.45 ± 0.04). These results support that the larger L-type current during the day was due to increased activation of the current at the peak, not differences in inactivation. Furthermore, inactivation of the N, P/Q, R, and T-type components did not vary diurnally (Fig. 3C).

The day versus night current properties were further probed by using SCN action potential waveforms to elicit $Ca^{2+}$ currents. These commands vary in the membrane potential and $t_{½}$ values (Fig. 4A), providing a mechanism for assessing the differences in $Ca^{2+}$ current during the typical spontaneous neuronal activity exhibited by SCN neurons. The action potential commands elicited measurable current responses from each subtype, showing the ability of single action potentials to activate $Ca^{2+}$ channels in SCN neurons. Similar to the peak current from standard voltage steps, the $Cd^{2+}$-sensitive current was larger from the daytime action potential command (Fig. 4B and C). Moreover, the ConoGVIA-, but not the Nimodipine-sensitive (−8 ± 1 and −7 ± 1 pA/pF), action potential-evoked currents were found to be larger during the day compared to night (Fig. 4C and D). In contrast, the $Ni^{2+}$-sensitive action potential-evoked current was actually higher at night (Fig. 4D). This suggests that under physiological conditions where a dynamic membrane voltage is encountered, the diurnal difference in $Ca^{2+}$ current subtypes may be more complex than predicted from step voltage commands.

Subthreshold membrane properties have also been reported to vary between day and night in SCN neurons (Pennartz et al., 2002). In current-clamp mode in the presence of TTX to block firing, 20% of cells exhibited spontaneous membrane potential oscillations during the day (n=10/48) compared to 8% at night (n=3/36) (Fig. 5A and B). When the membrane potential was varied between −60 and 0 mV, additional cells were able to generate oscillations (35%, n=17/48 during the day and 19%, n=7/36 at night). Consistent with previous observations (Pennartz et al., 2002; Jackson et al., 2004), no oscillations were observed in 10 μM Nimodipine (n=0/17 during the day and n=0/17 at night), implicating LTCCs as the source of the oscillation (Fig. 5A and B). These data demonstrate that SCN cells also displayed another aspect in the diurnal modulation of L-type $Ca^{2+}$ current. In addition to a diurnal difference in current magnitude in voltage-clamp, there are diurnal differences in spontaneous $Ca^{2+}$ channel activity that produce oscillatory membrane behavior.

Lastly, the mechanism of the diurnal difference in the macroscopic L-type current magnitude in voltage-clamp mode was investigated. To address whether L-type channels might be

removed from the cell membrane to produce the decrease in the Nimodipine-sensitive current observed at night, the sensitivity of the $Ca^{2+}$ current to the L-type agonist Bay K was assessed (Fig. 6). In this experiment, a reduction in L-type channels would result in a reduced effect of Bay K on the current magnitude. We found that Bay K increased the $Ca^{2+}$ current, both during the day and at night. This increased current was plotted as the Bay K-sensitive current (Fig. 6A–D). Notably, the Bay K-sensitive current was not different in magnitude of the peak, or the current-voltage relationship, between day and night (Fig. 6F). Even normalizing to the total $Ca^{2+}$ current to account for any cell to cell differences, Bay K still produced similar current ratios at both timepoints, increasing the current by 16 ± 4% during the day and 13± 2% during the night (Fig. 6F). Generally, the lack of a nighttime reduction in the Bay K-sensitive current suggests that nighttime channels can produce as much current as daytime channels, arguing against the idea that L-type channels are substantially removed from the membrane at night. Furthermore, because the relative L-type current magnitude is lower at night, the ratio of the Bay K current to the Nimodipine-sensitive current was actually enhanced at night (Fig. 6G).

## Role of VGCCs in SCN firing and rhythms

To identify which $Ca^{2+}$ channel subtypes are involved in action potential firing, and whether the same $Ca^{2+}$ channels affect action potential frequency during the day versus night, spontaneous action potential frequency was recorded in extracellular mode from acute SCN slices. During the day, SCN neuronal firing exhibited a significant decrease with pan-VGCC, L-, N-, P/Q-, and R-type channel inhibitors compared to daytime control ($Cd^{2+}$; −72 ± 9%; Nimodipine, −26 ± 9%; ConoGVIA, −64 ± 8%; AgaIVA, −68 ± 8%; and $Ni^{2+}$, −48 ± 8%) (Fig. 7A and B). In contrast, during the night, when firing rate is relatively low, the only VGCC inhibitor that significantly affected nighttime action potential frequency was the nonspecific VGCC inhibitor $Cd^{2+}$ (−60 ± 18%). Other VGCC inhibitors did not affect nighttime action potential frequency (Fig. 7A and C). TTAP2 did not significantly affect action potential frequency in either day or night, suggesting T-type $Ca^{2+}$ currents are not major mediators of action potential frequency in the SCN. These data identify that L-, N-, P/Q-, and R-type $Ca^{2+}$ channel contributions to spontaneous firing in SCN neurons are daytime-specific.

$Ca^{2+}$ channel subtypes that regulate action potential frequency at the cellular level have the potential to shape circadian rhythms in firing rate within the circuit. To test this, extracellular action potential activity from organotypic SCN slices grown on multi-electrode arrays were recorded continuously for 6 days. The day versus night difference in firing is manifest as a sinusoidal oscillation in frequency that is synchronized across the SCN. The number of recording electrodes within the SCN ranged from 9 to 28 for each slice. Rhythmic activity in the SCN was assessed from 3 days of baseline and compared to 3 days of activity in the presence of $Ca^{2+}$ channel inhibitors. Circadian parameters included the percentage of rhythmic recordings, period length, and rhythm amplitude (peak of the $\chi^2$ periodogram). Between slices, there is some variability in the frequency of the multi-unit activity recorded on MEAs. However, there were no significant differences in rhythmic parameters at baseline between the baseline controls, including the percentage of rhythmic recordings and $\chi^2$ amplitude of the circuit (Fig. 8G and H; $P>0.05$; One-way ANOVA). In addition, application

of a vehicle control (culture media alone, or culture media containing DMSO (<0.01%) had no effect on rhythmic parameters compared to baseline recordings (Fig. 8A, G–I). However, several VGCC inhibitors significantly decreased the rhythmicity of SCN firing activity. Compared to their respective baselines, the percentage of rhythmic recordings was decreased following the application of Nimodipine (−19±6%), ConoGVIA (−17±6%), AgaIVA (−28±5%) and $Ni^{2+}$ (−29±7%)(Fig. 8B–I). Consistent with this decrease in the number of rhythmic recordings, the circadian amplitude of the entire circuit ($\chi^2$ amplitude calculated from all electrodes within the SCN) was decreased after drug application for Nimodipine (−50±20%, P=0.04), ConoGVIA (−51±18%, P=0.04), AgaIVA (−63±14%, P=0.01), and $Ni^{2+}$ (−48±20%, P=0.04) compared to baseline. These data corroborate that alterations in neuronal firing rates lead to altered circuit rhythmicity.

To understand in greater detail whether the portion of circuit activity that remained rhythmic in the presence of each $Ca^{2+}$ channel inhibitor was normal, or whether this portion of the circuit activity also exhibited degraded rhythmicity, an additional analysis restricted to only the rhythmic recordings that persisted in the presence of the respective $Ca^{2+}$ channel inhibitors was conducted. This analysis revealed that the $\chi^2$ amplitude was similarly decreased in Nimodipine (−50±20%), ConoGVIA (−40±13%), AgaIVA (−47±14%) and $Ni^{2+}$ (−42±16%) compared to baseline (Fig. 8H). However, Nim, ConGVIA, AgaIVA, and $Ni^{2+}$ did not affect period length (Fig. 8I). Taken together, these data suggest that altered firing activity with inhibition of L-, N-, P/Q-, and R-type channels disrupts the robustness of the circadian rhythm (amplitude), but not the basic periodicity of the rhythm. In contrast, TTAP2 had no effect on the percentage of rhythmic recordings, circuit $\chi^2$ amplitude, rhythmic $\chi^2$ amplitude, or period length (Fig. 8G–I), consistent with the result that inhibition of T-type channels had no effect on extracellular action potential frequency during the day or night.

Since the L-type $Ca^{2+}$ current exhibits diurnal modulation in its levels, we also tested whether aberrant activation of L-type channels throughout the circadian cycle by application of Bay K would disrupt action potential rhythmicity as well. Bay K decreased the percentage of rhythmic recordings (−37±8%), $\chi^2$ amplitude of the entire circuit (−67±20%, P=0.04), and $\chi^2$ amplitude of the remaining rhythmic recordings (−62±19%) (Fig. 8G and H). However, Bay K had no effect on period length compared to baseline recordings (Fig. 8I). This result suggests that not only the function of L-type channels, but the diurnal modulation of current levels, may be required for maintaining proper circuit rhythm amplitude.

## Role of intracellular $Ca^{2+}$ channels in SCN firing and rhythms

Intracellular $Ca^{2+}$ channels do not produce membrane currents, but have previously been shown to be involved in modulating firing rate in SCN neurons (Aguilar-Roblero et al., 2007; Aguilar-Roblero et al., 2016; Whitt et al., 2018). We therefore tested the effects of blocking release of $Ca^{2+}$ from intracellular stores with two inhibitors. Dantrolene (Dan, 10 μM) is expected to selectively inhibit ryanodine receptors (RyRs)($IC_{50}$ = 0.16 μM for isoforms RyR1 and RyR2) and decrease $Ca^{2+}$-induced $Ca^{2+}$ release from intracellular stores by 50-60% (Oo et al., 2015). Cyclopiazonic acid (CPA, 10 μM), a selective and potent inhibitor of SERCA-ATPase, is expected to disrupt $Ca^{2+}$ re-uptake into the endoplasmic

reticulum and inhibit $Ca^{2+}$-induced $Ca^{2+}$ release from intracellular stores (de Juan-Sanz et al., 2017).

In this study, daytime action potential firing was slightly decreased in the presence of intracellular $Ca^{2+}$ channel inhibitors (Dan, −30 ± 9% and CPA −26 ± 9%)(Fig. 7A and B)). In contrast, nighttime firing increased in Dan (+101±15%) and CPA (+122±16%) (Fig. 7A and C). This data shows that unlike VGCC subtypes, which have daytime-specific effects on firing, intracellular $Ca^{2+}$ channels (RyRs), or intracellular $Ca^{2+}$ stores can influence action potential firing in both day and night.

Despite the effect of Dan and CPA on extracellular action potential frequency in acute SCN slices, these inhibitors had no effect on the percentage of rhythmic recordings or the $\chi^2$ amplitude of the circuit (Fig. 8G and H). However, Dan did increase the period length by 1.5±0.5 hrs compared to baseline (Fig. 8I). CPA application did not corroborate the effect on period, raising the possibility that homeostatic regulatory mechanisms controlling intracellular $Ca^{2+}$ , or a resulting disruption of endoplasmic reticulum protein processing, may be engaged with the chronic depletion of intracellular $Ca^{2+}$ stores over 3 days with CPA treatment. This possibility may also factor into the discrepancy between the acute effects of Dan on firing rate, which is to reduce firing during the day and increase it at night, and the effect of chronic treatment over 3 cycles in MEA recordings. Thus, although it is clear that intracellular $Ca^{2+}$ channels regulate firing, their role in rhythmicity is still less than conclusive.

## DISCUSSION

In this study, we used whole-cell and extracellular electrophysiological recordings to define the inward L-, N-, P/Q-, R-, and T-type $Ca^{2+}$ currents present in SCN neurons during the day and night and their role in action potential firing. Macroscopic currents showed significant heterogeneity in magnitude for each subtype and variability in the relative contribution to the total $Ca^{2+}$ current at both times of the cycle. Although it was previously shown that the L-type current magnitude, and nimodipine-sensitive subthreshold membrane potential oscillations, are greater during the day in SCN neurons (Pennartz et al., 2002; Whitt et al., 2018), it was not clear whether other $Ca^{2+}$ current subtypes also exhibited circadian regulation and how much each subtype contributes to the total $Ca^{2+}$ current, or modulation of firing rate, between day and night. We found that L-, N-, P/Q-, and R-type $Ca^{2+}$ currents broadly facilitate the higher frequency spontaneous firing observed in daytime SCN neurons, with little effect at night. Furthermore, although $Ni^{2+}$-sensitive currents comprised the largest proportion of total VGCC current, the currents did not grossly vary in magnitude between day and night, suggesting R-type currents are not circadianly regulated. There is no evidence that N- or P/Q-type $Ca^{2+}$ currents are circadianly regulated either. Although it was reported that T-type currents were larger in early night in retinorecipient SCN neurons (Kim et al., 2005), these currents were rare and a diurnal difference was not broadly established in the general population of SCN neurons in this study. The systematic interrogation under the same conditions support the conclusion that the underlying circadian modulation of the L-type $Ca^{2+}$ current is singular among the different subtypes, despite the similarly daytime-restricted roles for N-, P/Q-, and R-type channels in facilitating action potential firing. This

finding raises important questions concerning how rhythmic firing is produced, challenging assumptions that the contributing channel components must be distinct in their current levels between day and night.

In this study and others, Nimodipine-sensitive $Ca^{2+}$ current is about twice as large during the day compared to night (Pennartz et al., 2002; Whitt et al., 2018). The mechanism of the underlying circadian regulation of the L-type current is not yet known. Although L-type transcripts had the highest abundance in SCN among the different subtypes (Nahm et al., 2005), there is no definitive evidence demonstrating a daytime-phase increase in Cav1-family channel transcript or protein expression, which underlie the L-type current. Two L-type channel subtypes (Cav1.2 and Cav1.3) are expressed in the SCN (Nahm et al., 2005) and are subject to transcriptional regulation via alternative splicing (Cav1.2)(Partridge & Carter, 2017) and RNA-editing (Cav1.3)(Huang H, 2012). However, Cav1.2 has incongruently been reported to peak during the late night (Schmutz et al., 2014), not during the day when current magnitude is highest. Related to this, we found that Bay K, a selective agonist of L-type channels, could increase nighttime current to the same levels as day. A simple interpretation of this data is that the nighttime decrease in L-type current is not due to a significant reduction in L-type channels on the membrane at night, which would be expected to reduce the effect of Bay K. There is a similar incongruence with the expression profile for other transcripts also failing to match the lack of day versus night difference in current levels. For example, P/Q- and T-type channels expression exhibit peaks at CT12 (Nahm et al., 2005). The discrepancies reveal the need for more detailed studies addressing molecular basis for the diurnal modulation of $Ca^{2+}$ current levels and how the time-of-day specific roles in action potential firing are produced.

Cav1.3 could also contribute to the L-type current. Cav1.3 transcripts have been proposed to undergo RNA editing in SCN, a modification which affects $Ca^{2+}$-dependent inactivation (Huang H, 2012). Experiments presented here corroborate previous work showing the daytime increase was observed in the peak current activation and was not due to circadian changes in channel inactivation (Pennartz et al., 2002), suggesting a potential role for Cav1.3 editing may be to contribute to another aspect of channel function besides the diurnal regulation of current levels. One speculative role for Cav1.3 channels would be to generate the nimodipine-sensitive subthreshold membrane potential oscillations, as has been demonstrated for Cav1.3 channels in other cell types (Platzer et al., 2000; Vandael et al., 2015).

The data in this study data connect alterations in neuronal firing rates to changes in circuit rhythmicity, a major output signal of the SCN. Nimodipine, ConoGVIA, AgaIVA and $Ni^{2+}$ decreased rhythmicity, but did not affect the period of the rhythm, suggesting L-, N-, P/Q-, and R-type channels regulate SCN output but not the core clock time-encoding function. This finding is notable because it suggests that rhythmic current modulation is not required for certain $Ca^{2+}$ channel subtypes to regulate circuit rhythmicity. Yet application of the L-type $Ca^{2+}$ channel activator BayK, which increased nighttime current levels, had a similar effect on firing rhythms when compared to Nimodipine. The latter result would suggest that, at least for L-type current, the day versus night current level is important for SCN rhythmicity.

Additional evidence from animal studies also links specific $Ca^{2+}$ channels with SCN outputs and behaviors. Genetic knockout of Cav1.2 reduced the ability of rats to adapt their behavioral rhythms, as well as clock gene *Per1* expression, to light-induced phase advances (Schmutz et al., 2014). Nimodipine also abolished glutamate-induced phase advances in SCN slices (Kim et al., 2005). Moreover, genetic knockout of Cav2.2 (N-type channel) in mice caused behavioral hyperactivity and decreased sleep (Beuckmann et al., 2003). N-type channel antagonists abolished circadian rhythms in drinking behavior in rats (Masutani et al., 1995). P/Q-type channels have been shown to regulate GABA release, the major neurotransmitter in SCN (Chen & van den Pol, 1998). Genetic knockout of Cav3.1 (T-type channels) altered sleep/wake periods in mice (Lee et al., 2004). These studies suggest the $Ca^{2+}$ channels that regulate firing rate and rhythmicity are also implicated in behaviors regulated by the circadian clock.

Intracellular RyR $Ca^{2+}$ channels have also implicated in clock output. RyR activation with 100 nM ryanodine *in vivo* shortened the period of locomotor activity in rats (Ding et al., 1998; Mercado et al., 2009). Dysregulation of cytosolic $Ca^{2+}$ homeostasis has furthermore been proposed to contribute to age-related deterioration of clock function (Farajnia et al., 2015). However, from this study and others, it is less clear how $Ca^{2+}$ release from intracellular stores contributes to SCN rhythmicity. RyR isoforms 1 and 2 (RyR1 and RyR2) have been identified in the SCN (Diaz-Munoz et al., 1999). RyR2 is the most abundantly expressed isoform, and RyR2 mRNA and protein are more highly expressed during the day (Diaz-Munoz et al., 1999; Pfeffer et al., 2009). However, inhibition of RyRs with Dan affected firing at both times of day. Unexpectedly, at the circuit level, this inhibitor had only a minor effect on action potential firing rhythms, suggesting the regulation of intracellular $Ca^{2+}$ in SCN neurons is tightly controlled and disruptions in $Ca^{2+}$ homeostasis are compensated for over time. This is the first study examining the effects of Dan for over a full circadian cycle. This evidence could suggest the changes in firing due to Dan are transient.

At least one membrane target connecting RyR $Ca^{2+}$ release to the plasma membrane channels that regulate action potential activity has been identified, the BK $Ca^{2+}$-activated $K^{+}$ channel (Whitt et al., 2018). BK channels require RyRs for their $Ca^{2+}$-dependent activation only at night. The increase in nighttime firing with Dan observed in acute slices, and elongation of the SCN firing period in organotypic slices is similar to results obtained with BK channel inhibitors (Meredith et al., 2006; Kent & Meredith, 2008). However, BK channel inhibition also produces a significant decrease in the percent of rhythmic recordings and decreased circadian amplitudes in MEA experiments (Kent & Meredith, 2008) that were not observed here. One potential explanation for the difference could be that chronic application of Dan, and the SERCA inhibitor CPA, caused homeostatic compensation in intracellular $Ca^{2+}$ that precluded evaluating their long-term effects on firing. Additional experiments will be required to conclusively determine the role of RyRs in SCN firing rhythms, but such a role is suggested by the behavioral data.

In summary, we comprehensively assessed which currents had evidence for diurnal regulation, and the role of these subtypes in SCN action potential firing and rhythmicity. We found that diurnal regulation of macroscopic current magnitude was not a universal feature required to produce an effect on the circadian regulation of firing. Identification of L-type

$Ca^{2+}$ channels, and unexpectedly N-, P/Q- and R-type channels as well, as necessary for SCN circuit rhythmicity, provides a new basis for the further investigation of their mechanisms for action potential regulation.

## ACKNOWLEDGEMENTS

We thank Ivy Dick for helpful advice and comments on the manuscript.

FUNDING

This work was supported by grants from NHLBI R01-HL102758 (A.L.M.) and The American Physiological Society's Ryuji Ueno award, sponsored by the S & R Foundation (A.L.M.). A.L.M. and A.E.P. were supported by NIGMS T32-GM008181.

## REFERENCES

Aguilar-Roblero R, Mercado C, Alamilla J, Laville A & Diaz-Munoz M. (2007). Ryanodine receptor $Ca^{2+}$-release channels are an output pathway for the circadian clock in the rat suprachiasmatic nuclei. Eur J Neurosci 26, 575–582. [PubMed: 17686038]

Aguilar-Roblero R, Quinto D, Baez-Ruiz A, Chavez JL, Belin AC, Diaz-Munoz M, Michel S & Lundkvist G. (2016). Ryanodine-sensitive intracellular $Ca^{2+}$ channels are involved in the output from the SCN circadian clock. Eur J Neurosci 44, 2504–2514. [PubMed: 27529310]

Beuckmann CT, Sinton CM, Miyamoto N, Ino M & Yanagisawa M. (2003). N-type calcium channel alpha1B subunit (Cav2.2) knock-out mice display hyperactivity and vigilance state differences. J Neurosci 23, 6793–6797. [PubMed: 12890773]

Boland LM, Morrill JA & Bean BP. (1994). omega-Conotoxin block of N-type calcium channels in frog and rat sympathetic neurons. J Neurosci 14, 5011–5027. [PubMed: 8046465]

Chen G & van den Pol AN. (1998). Presynaptic GABAB autoreceptor modulation of P/Q-type calcium channels and GABA release in rat suprachiasmatic nucleus neurons. J Neurosci 18, 1913–1922. [PubMed: 9465016]

Cloues RK & Sather WA. (2003). Afterhyperpolarization regulates firing rate in neurons of the suprachiasmatic nucleus. J Neurosci 23, 1593–1604. [PubMed: 12629163]

de Jeu M, Hermes M & Pennartz C. (1998). Circadian modulation of membrane properties in slices of rat suprachiasmatic nucleus. Neuroreport 9, 3725–3729. [PubMed: 9858386]

de Juan-Sanz J, Holt GT, Schreiter ER, de Juan F, Kim DS & Ryan TA. (2017). Axonal Endoplasmic Reticulum $Ca^{2+}$ Content Controls Release Probability in CNS Nerve Terminals. Neuron 93, 867–881 e866. [PubMed: 28162809]

Diaz-Munoz M, Dent MA, Granados-Fuentes D, Hall AC, Hernandez-Cruz A, Harrington ME & Aguilar-Roblero R. (1999). Circadian modulation of the ryanodine receptor type 2 in the SCN of rodents. Neuroreport 10, 481–486. [PubMed: 10208575]

Ding JM, Buchanan GF, Tischkau SA, Chen D, Kuriashkina L, Faiman LE, Alster JM, McPherson PS, Campbell KP & Gillette MU. (1998). A neuronal ryanodine receptor mediates light-induced phase delays of the circadian clock. Nature 394, 381–384. [PubMed: 9690474]

Dreyfus FM, Tscherter A, Errington AC, Renger JJ, Shin HS, Uebele VN, Crunelli V, Lambert RC & Leresche N. (2010). Selective T-type calcium channel block in thalamic neurons reveals channel redundancy and physiological impact of I(T)window. J Neurosci 30, 99–109. [PubMed: 20053892]

Farajnia S, Meijer JH & Michel S. (2015). Age-related changes in large-conductance calcium-activated potassium channels in mammalian circadian clock neurons. Neurobiology of aging 36, 2176–2183. [PubMed: 25735218]

Flourakis M & Allada R. (2015). Patch-clamp electrophysiology in *Drosophila* circadian pacemaker neurons. Methods Enzymol 552, 23–44. [PubMed: 25707271]

Hamada T, Niki T, Ziging P, Sugiyama T, Watanabe S, Mikoshiba K & Ishida N. (1999). Differential expression patterns of inositol trisphosphate receptor types 1 and 3 in the rat suprachiasmatic nucleus. Brain Res 838, 131–135. [PubMed: 10446325]

Hermanstyne TO, Granados-Fuentes D, Mellor RL, Herzog ED & Nerbonne JM. (2017). Acute Knockdown of Kv4.1 Regulates Repetitive Firing Rates and Clock Gene Expression in the Suprachiasmatic Nucleus and Daily Rhythms in Locomotor Behavior. eNeuro 4.

Huang H TB, Shen Y, Tao J, Jiang F, Sung YY, Ng CK, Raida M, Köhr G, Higuchi M, Fatemi-Shariatpanahi H, Harden B, Yue DT, Soong TW. (2012). RNA editing of the IQ domain in $Ca_V1.3$ channels modulates their $Ca^{2+}$-dependent inactivation. Neuron 73, 304–316. [PubMed: 22284185]

Ikeda M, Sugiyama T, Wallace CS, Gompf HS, Yoshioka T, Miyawaki A & Allen CN. (2003). Circadian dynamics of cytosolic and nuclear $Ca^{2+}$ in single suprachiasmatic nucleus neurons. Neuron 38, 253–263. [PubMed: 12718859]

Itri JN, Vosko AM, Schroeder A, Dragich JM, Michel S & Colwell CS. (2010). Circadian regulation of a-type potassium currents in the suprachiasmatic nucleus. J Neurophysiol 103, 632–640. [PubMed: 19939959]

Itri JN, Michel S, Vansteensel MJ, Meijer JH & Colwell CS. (2005). Fast delayed rectifier potassium current is required for circadian neural activity. Nat Neurosci 8, 650–656. [PubMed: 15852012]

Jackson AC, Yao GL & Bean BP. (2004). Mechanism of spontaneous firing in dorsomedial suprachiasmatic nucleus neurons. J Neurosci 24, 7985–7998. [PubMed: 15371499]

Kent J & Meredith AL. (2008). BK channels regulate spontaneous action potential rhythmicity in the suprachiasmatic nucleus. PLoS One 3, e3884. [PubMed: 19060951]

Kim DY, Choi HJ, Kim JS, Kim YS, Jeong DU, Shin HC, Kim MJ, Han HC, Hong SK & Kim YI. (2005). Voltage-gated calcium channels play crucial roles in the glutamate-induced phase shifts of the rat suprachiasmatic circadian clock. Eur J Neurosci 21, 1215–1222. [PubMed: 15813931]

Kuhlman SJ & McMahon DG. (2006). Encoding the ins and outs of circadian pacemaking. J Biol Rhythms 21, 470–481. [PubMed: 17107937]

Lee J, Kim D & Shin HS. (2004). Lack of delta waves and sleep disturbances during non-rapid eye movement sleep in mice lacking alpha1G-subunit of T-type calcium channels. Proc Natl Acad Sci U S A 101, 18195–18199. [PubMed: 15601764]

Lee JH, Gomora JC, Cribbs LL & Perez-Reyes E. (1999). Nickel block of three cloned T-type calcium channels: low concentrations selectively block alpha1H. Biophys J 77, 3034–3042. [PubMed: 10585925]

Lehman MN, Silver R, Gladstone WR, Kahn RM, Gibson M & Bittman EL. (1987). Circadian rhythmicity restored by neural transplant. Immunocytochemical characterization of the graft and its integration with the host brain. J Neurosci 7, 1626–1638. [PubMed: 3598638]

Lewis RJ, Nielsen KJ, Craik DJ, Loughnan ML, Adams DA, Sharpe IA, Luchian T, Adams DJ, Bond T, Thomas L, Jones A, Matheson JL, Drinkwater R, Andrews PR & Alewood PF. (2000). Novel omega-conotoxins from Conus catus discriminate among neuronal calcium channel subtypes. J Biol Chem 275, 35335–35344. [PubMed: 10938268]

Marchetti C, Amico C & Usai C. (1995). Functional characterization of the effect of nimodipine on the calcium current in rat cerebellar granule cells. J Neurophysiol 73, 1169–1180. [PubMed: 7608763]

Masutani H, Matsuda Y, Nagai K & Nakagawa H. (1995). Effect of Ω-conotoxin, a calcium channel blocker, on the circadian rhythm in rats. Biological Rhythm Research 26, 573–581.

McDonough SI, Swartz KJ, Mintz IM, Boland LM & Bean BP. (1996). Inhibition of calcium channels in rat central and peripheral neurons by omega-conotoxin MVIIC. J Neurosci 16, 2612–2623. [PubMed: 8786437]

Mercado C, Diaz-Munoz M, Alamilla J, Valderrama K, Morales-Tlalpan V & Aguilar-Roblero R. (2009). Ryanodine-sensitive intracellular $Ca^{2+}$ channels in rat suprachiasmatic nuclei are required for circadian clock control of behavior. J Biol Rhythms 24, 203–210. [PubMed: 19465697]

Meredith AL, Wiler SW, Miller BH, Takahashi JS, Fodor AA, Ruby NF & Aldrich RW. (2006). BK calcium-activated potassium channels regulate circadian behavioral rhythms and pacemaker output. Nat Neurosci 9, 1041–1049. [PubMed: 16845385]

Mintz IM, Venema VJ, Swiderek KM, Lee TD, Bean BP & Adams ME. (1992). P-type calcium channels blocked by the spider toxin omega-Aga-IVA. Nature 355, 827–829. [PubMed: 1311418]

Montgomery JR, Whitt JP, Wright BN, Lai MH & Meredith AL. (2013). Mis-expression of the BK $K^+$ channel disrupts suprachiasmatic nucleus circuit rhythmicity and alters clock-controlled behavior. Am J Physiol Cell Physiol 304, C299–311. [PubMed: 23174562]

Moore RY & Eichler VB. (1972). Loss of a circadian adrenal corticosterone rhythm following suprachiasmatic lesions in the rat. Brain Res 42, 201–206. [PubMed: 5047187]

Nahm SS, Farnell YZ, Griffith W & Earnest DJ. (2005). Circadian regulation and function of voltage-dependent calcium channels in the suprachiasmatic nucleus. J Neurosci 25, 9304–9308. [PubMed: 16207890]

Newcomb R, Szoke B, Palma A, Wang G, Chen X, Hopkins W, Cong R, Miller J, Urge L, Tarczy-Hornoch K, Loo JA, Dooley DJ, Nadasdi L, Tsien RW, Lemos J & Miljanich G. (1998). Selective peptide antagonist of the class E calcium channel from the venom of the tarantula Hysterocrates gigas. Biochemistry 37, 15353–15362. [PubMed: 9799496]

Nitabach MN, Holmes TC & Blau J. (2005). Membranes, ions, and clocks: testing the njus-sulzman-hastings model of the circadian oscillator. Methods Enzymol 393, 682–693. [PubMed: 15817319]

Oo YW, Gomez-Hurtado N, Walweel K, van Helden DF, Imtiaz MS, Knollmann BC & Laver DR. (2015). Essential Role of Calmodulin in RyR Inhibition by Dantrolene. Mol Pharmacol 88, 57–63. [PubMed: 25920678]

Partridge LMM, Carter DA (2017). Novel Rbfox2 isoforms associated with alternative exon usage in rat cortex and suprachiasmatic nucleus. Sci Rep. 7, 9929. [PubMed: 28855650]

Pennartz CM, de Jeu MT, Bos NP, Schaap J & Geurtsen AM. (2002). Diurnal modulation of pacemaker potentials and calcium current in the mammalian circadian clock. Nature 416, 286–290. [PubMed: 11875398]

Pfeffer M, Muller CM, Mordel J, Meissl H, Ansari N, Deller T, Korf HW & von Gall C. (2009). The mammalian molecular clockwork controls rhythmic expression of its own input pathway components. J Neurosci 29, 6114–6123. [PubMed: 19439589]

Platzer J, Engel J, Schrott-Fischer A, Stephan K, Bova S, Chen H, Zheng H & Striessnig J. (2000). Congenital deafness and sinoatrial node dysfunction in mice lacking class D L-type $Ca^{2+}$ channels. Cell 102, 89–97. [PubMed: 10929716]

Randall A & Tsien RW. (1995). Pharmacological dissection of multiple types of $Ca^{2+}$ channel currents in rat cerebellar granule neurons. J Neurosci 15, 2995–3012. [PubMed: 7722641]

Schmutz I, Chavan R, Ripperger JA, Maywood ES, Langwieser N, Jurik A, Stauffer A, Delorme JE, Moosmang S, Hastings MH, Hofmann F & Albrecht U. (2014). A specific role for the REV-ERBalpha-controlled L-Type Voltage-Gated Calcium Channel CaV1.2 in resetting the circadian clock in the late night. J Biol Rhythms 29, 288–298. [PubMed: 25238857]

Stephan FK & Zucker I. (1972). Circadian rhythms in drinking behavior and locomotor activity of rats are eliminated by hypothalamic lesions. Proc Natl Acad Sci U S A 69, 1583–1586. [PubMed: 4556464]

Talley EM, Cribbs LL, Lee JH, Daud A, Perez-Reyes E & Bayliss DA. (1999). Differential distribution of three members of a gene family encoding low voltage-activated (T-type) calcium channels. J Neurosci 19, 1895–1911. [PubMed: 10066243]

Tottene A, Moretti A & Pietrobon D. (1996). Functional diversity of P-type and R-type calcium channels in rat cerebellar neurons. J Neurosci 16, 6353–6363. [PubMed: 8815914]

Vandael DH, Marcantoni A & Carbone E. (2015). Cav1.3 Channels as Key Regulators of Neuron-Like Firings and Catecholamine Release in Chromaffin Cells. Curr Mol Pharmacol 8, 149–161. [PubMed: 25966692]

Whitt JP, McNally BA & Meredith AL. (2018). Differential contribution of $Ca^{2+}$ sources to day and night BK current activation in the circadian clock. J Gen Physiol 150, 259–275. [PubMed: 29237755]

Whitt JP, Montgomery JR & Meredith AL. (2016). BK channel inactivation gates daytime excitability in the circadian clock. Nature communications 7, 10837.

Yamazaki S, Kerbeshian MC, Hocker CG, Block GD & Menaker M. (1998). Rhythmic properties of the hamster suprachiasmatic nucleus in vivo. J Neurosci 18, 10709–10723. [PubMed: 9852606]

Zamponi GW, Bourinet E & Snutch TP. (1996). Nickel block of a family of neuronal calcium channels: subtype- and subunit-dependent action at multiple sites. J Membr Biol 151, 77–90. [PubMed: 8661496]

**Key Points Summary**

- Circadian oscillations in spontaneous action potential firing in the suprachiasmatic nucleus (SCN) translates time-of-day throughout the mammalian brain.
- The ion channels that regulate the circadian pattern of SCN firing have not been comprehensively identified.
- $Ca^{2+}$ channels regulate action potential activity across many types of excitable cells, and the activity of L-, N-, P/Q-, R-type channels are required for normal daytime firing frequency in SCN neurons and circuit rhythms.
- Only the L-type $Ca^{2+}$current exhibits a day versus night difference in current magnitude, providing insight into the mechanism which produces rhythmic action potential firing in SCN.

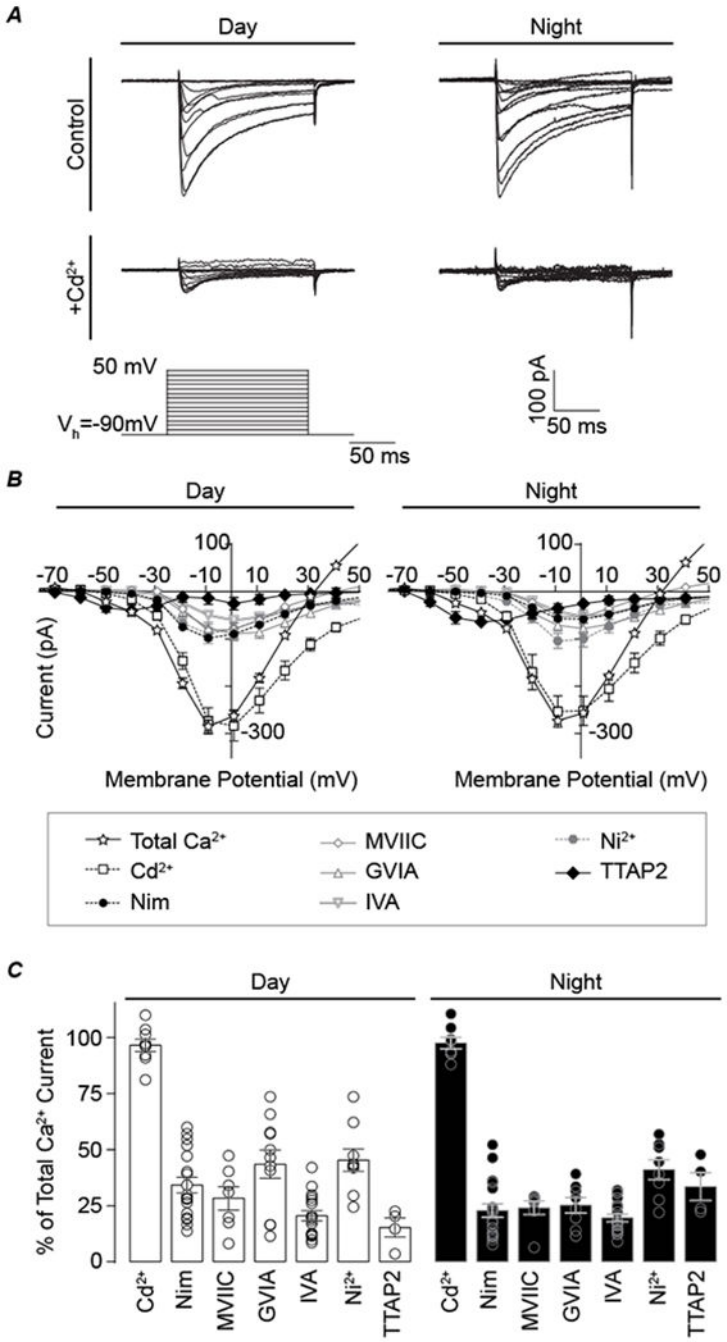


**Figure 1. Relative contribution of voltage-gated calcium currents in the SCN.**

Macroscopic voltage-activated calcium currents recorded in whole-cell voltage-clamp mode during the day or night. From a holding potential of −90 mV, currents were elicited from 150-ms voltage steps in 10-mV increments. *A*, Representative total $Ca^{2+}$ currents before (control) and after addition of $Cd^{2+}$. *B*, Current-voltage relationships for the total $Ca^{2+}$ current and $Cd^{2+}$-sensitive components, versus L-, N-, P/Q-, R-, and T-type subtypes of the $Ca^{2+}$ current ($Cd^{2+}$-sensitive, 200 μM; Nimodipine-sensitive, 10 μM; ConoMVIIC-sensitive, 3 μM; ConoGVIA-sensitive, 3 μM; AgaIVA-sensitive, 200 nM; $Ni^{2+}$-sensitive, 30 μM; and

TTAP2-sensitive, 1 μM). One $Ca^{2+}$ current subtype was isolated per cell by application of an inhibitor and subtraction from the baseline current (total $Ca^{2+}$). *C*, The relative contribution of each inhibitor-sensitive current to the total $Ca^{2+}$ current in day and night, calculated from the peak current. Due to the variation in current magnitudes from cell to cell (and overlapping specificities of the drugs), the sum of the individual inhibitors exceeds 100%. N's are the number of neurons recorded (day, night): $Cd^{2+}$ (12, 10), Nimodipine, (21, 20), ConoMVIIC (7, 7), ConoGVIA (11, 8), AgaIVA (17, 18), $Ni^{2+}$ (9, 8), TTAP2 (4, 4). Data were obtained from 3–8 slices per condition as follows (# slices day, # slices night): $Cd^{2+}$ (3, 3), Nimodipine, (8, 8), ConoMVIIC (2, 2), ConoGVIA (4, 4), AgaIVA (7, 6), $Ni^{2+}$ (3, 3), TTAP2 (2, 4). Total $Ca^{2+}$currents were obtained at baseline from all recordings (n=96 neurons in 35 slices for day and 82 neurons in 33 slices for night).

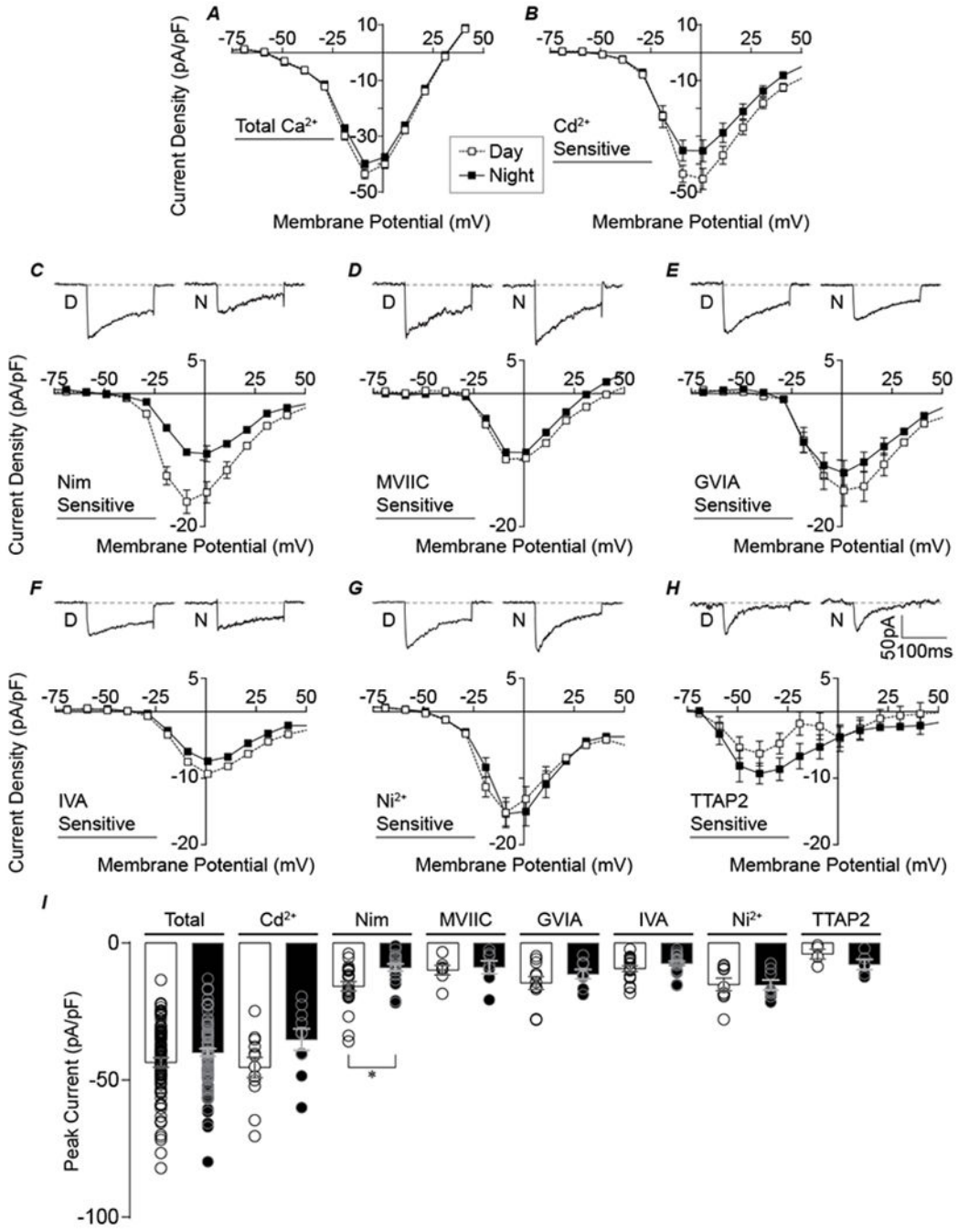


**Figure 2. Daytime $Cd^{2+}$- and Nimodipine-sensitive currents are larger than nighttime currents.**

*A-B*, Normalized day and night current density versus voltage relationships for total $Ca^{2+}$ (*A*) and $Cd^{2+}$ -sensitive (*B*) currents. *C-H*, Top panels: Representative peak currents for each subtype at voltages indicated in parentheses. Bottom panels: Normalized day and night current density versus voltage relationships. (*C*) Nimodipine-sensitive (−10 and 0 mV for day and night currents, respectively), (*D*) ConoMVIIC-sensitive (−10 mV, 0 mV), (*E*) ConoGVIA-sensitive (0 mV, 0 mV), (*F*) IVA-sensitive (0 mV, 0 mV), (*G*) $Ni^{2+}$ -sensitive (−10 mV, −10 mV), and (*H*) TTA-P2-sensitive currents (−40 mV, −40 mV). *I*, Summary

graph of peak current density for day (open bar) and night (filled bar) for all inhibitors in *A-H*. N's for each condition are the number of neurons recorded and are identical to Figure 1. *The day versus night Nimodipine-sensitive current was significantly different (P=0.002, respectively; unpaired *t*-test).

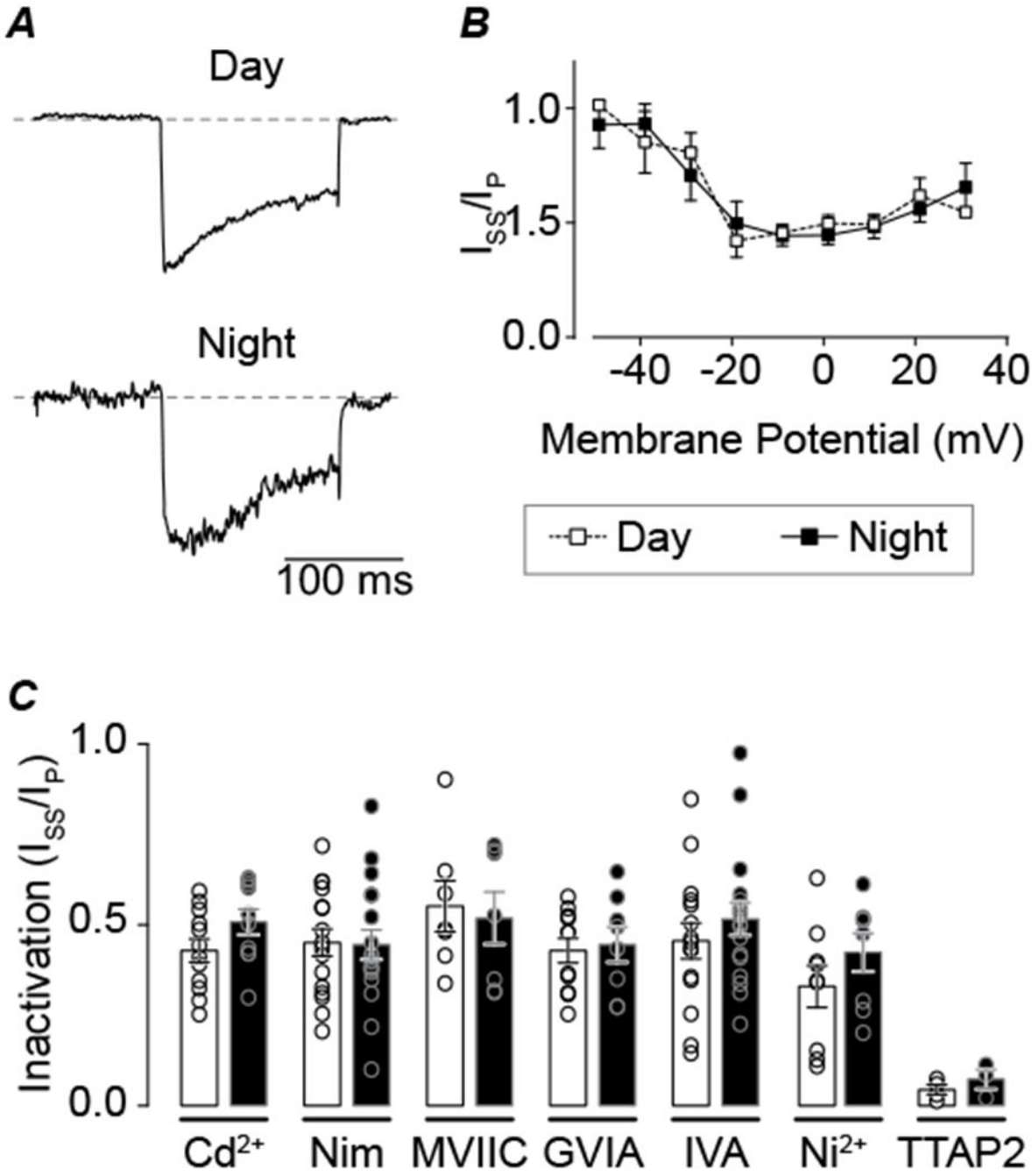


**Figure 3. Comparison of macroscopic inactivation between day and night for different $Ca^{2+}$ current subtypes.**

*A*, Nimodipine-sensitive current inactivation from day and night SCN cells. Representative day and night traces at −10 mV, with equivalently scaled peaks to compare the macroscopic current decay. *B*, Voltage-dependence of inactivation (steady-state current ($I_{SS}$) at 150 ms divided by peak current ($I_P$) for day and night Nimodipine-sensitive $Ca^{2+}$ currents. *C*, Summary of inactivation ratio for all VGCC subtypes. Current levels were taken from the peak voltage for each current (as in Fig. 2I). No significant differences between day and night were observed for any drug (unpaired *t*-test). N's are the number of neurons recorded

(day, night): $Cd^{2+}$-sensitive current (n=12, 10), Nimodipine-sensitive (16, 18), ConoMVIIC-sensitive (7, 7), ConoGVIA-sensitive (11, 8), AgaIVA-sensitive (15, 17), $Ni^{+}$-sensitive (9, 8), and TTAP2-sensitive (4, 3). Data were obtained from 2–8 slices per condition as follows (# slices day, # slices night): $Cd^{2+}$ (3, 3), Nimodipine, (8, 8), ConoMVIIC (2, 2), ConoGVIA (5, 5), AgaIVA (7, 7), $Ni^{2+}$ (4, 4), TTAP2 (2, 3).

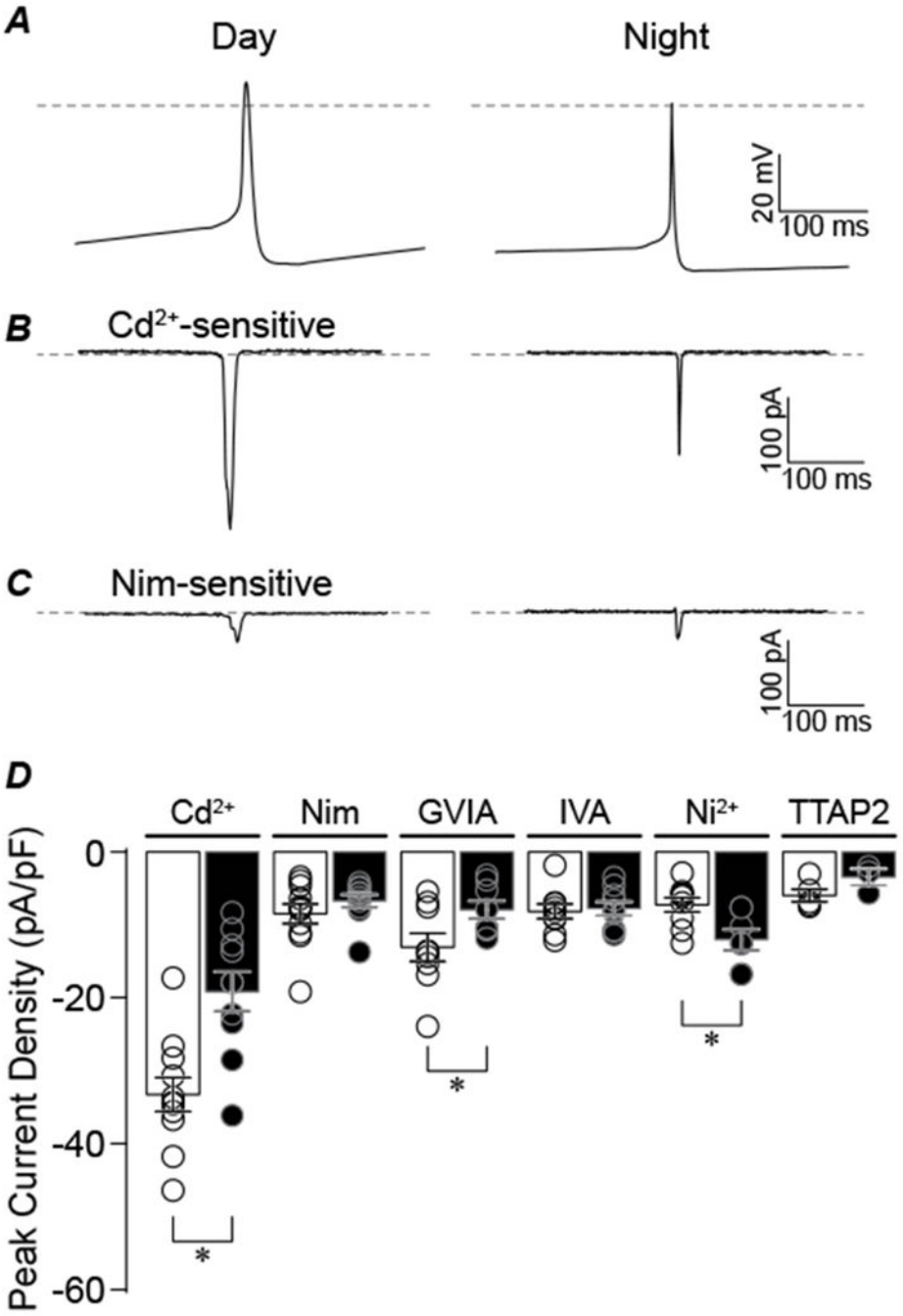


**Figure 4. Action potential evoked $Ca^{2+}$ currents from day and night SCN cells.**

*A*, Action potential voltage commands recorded from SCN neurons during the day and night were used to evoke $Ca^{2+}$ currents. Action potential commands were delivered from a holding potential of −150 mV. Dotted lines represent 0 mV. *B-C*, Representative day and night $Cd^{2+}$-sensitive (*B*) and Nimodipine-sensitive (*C*) current responses. *D*, Normalized peak current density for each $Ca^{2+}$ current subtype. *The day versus night $Cd^{2+}$-, ConoGVIA, and $Ni^{2+}$-sensitive currents are significantly different (P=0.001, P=0.04, and P=0.001, respectively; unpaired *t*-test). N's are the number of neurons recorded: $Cd^{2+}$-sensitive current (n=11 day,

10 night), Nimodipine-sensitive (11, 10), ConoGVIA-sensitive (9, 8), AgaIVA-sensitive (9, 9), $Ni^{+}$-sensitive (9, 7), and TTAP2-sensitive (5, 3). Data were obtained from 3–4 slices per condition as follows (# slices day, # slices night): $Cd^{2+}$ (3, 3), Nimodipine, (4, 4), ConoGVIA (3, 4), AgaIVA (3, 3), $Ni^{2+}$ (3, 4), TTAP2 (3, 3).

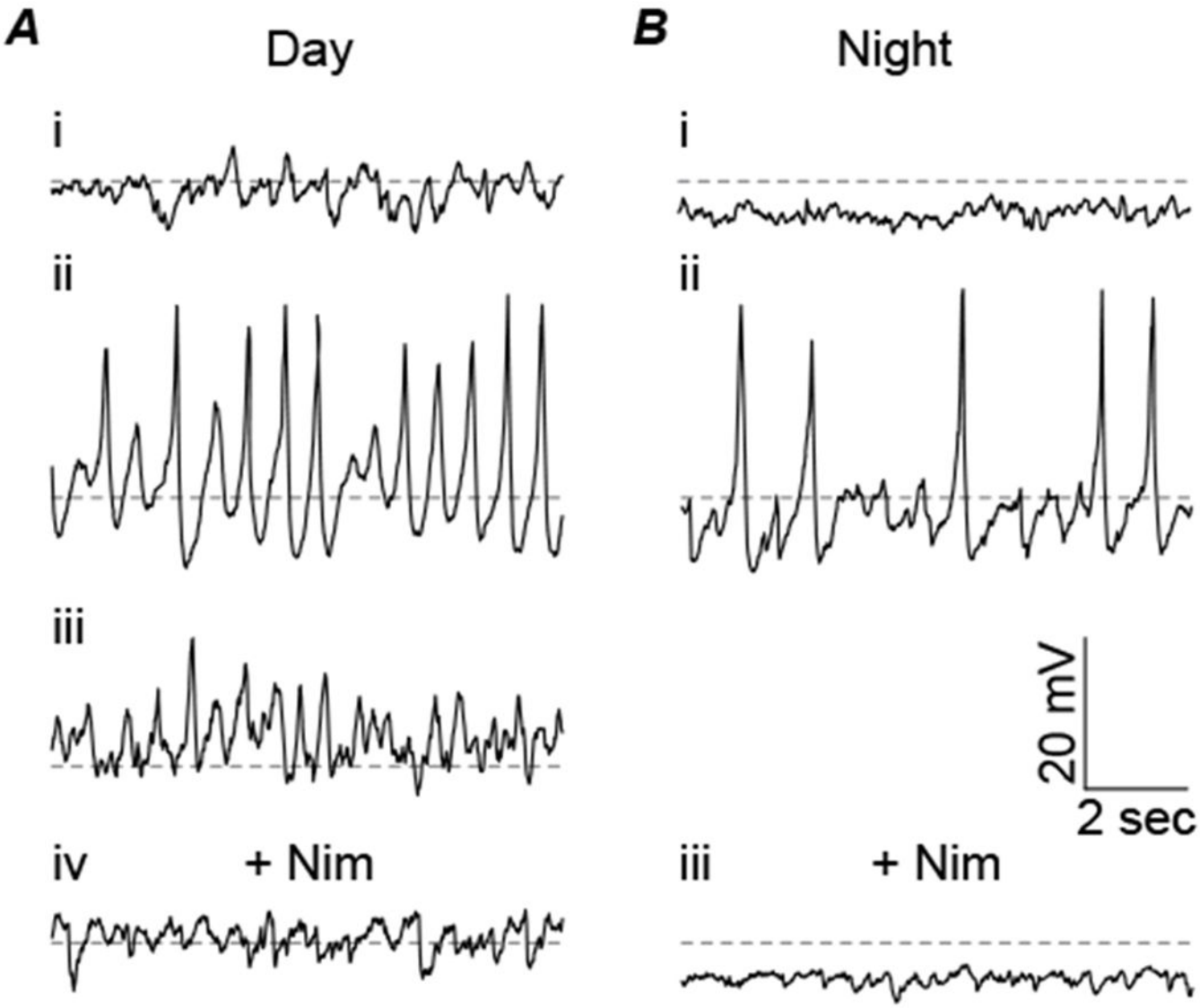


**Figure 5. Spontaneous $Ca^{2+}$ oscillations in day and night SCN cells.**

Subthreshold membrane potential oscillations recorded in whole-cell current-clamp mode in 1 μM TTX. *A*, Representative daytime membrane potential traces for a non-oscillating cell example (i) and two types of spontaneously oscillating cells (ii & iii). *B*, Representative nighttime membrane potential traces for a non-oscillating cell (i) and a spontaneously oscillating cell (ii). Nimodipine (10 μM) eliminated all spontaneous oscillations during the day (*A*iv) and the night (*B*iii).

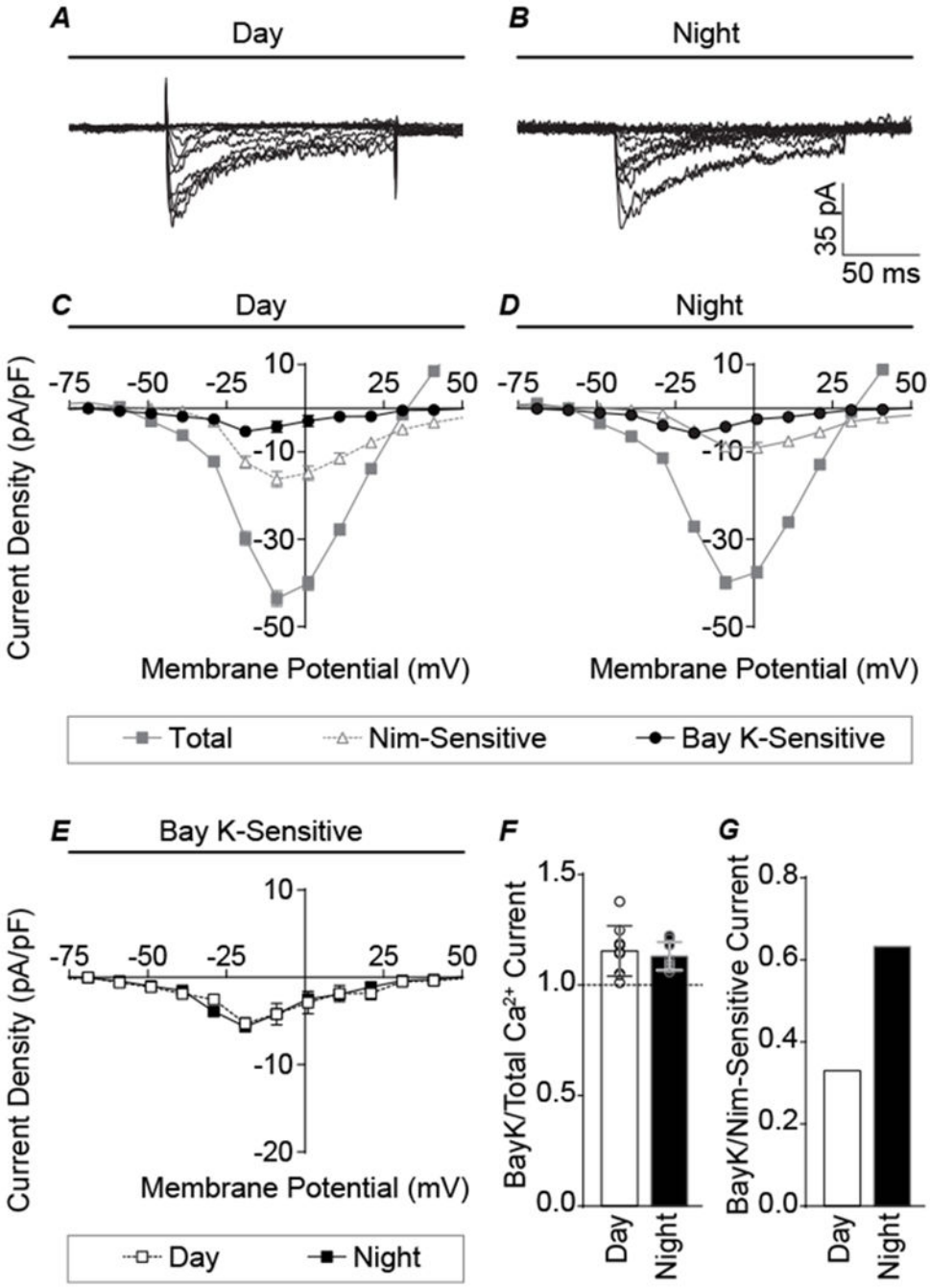


**Figure 6. Effects of Bay K8644 on $Ca^{2+}$ current during the day and night.**

*A-B*, Representative day and night Bay K-sensitive $Ca^{2+}$ currents. *C-D*, Current-voltage relationships for day and night total $Ca^{2+}$ current components. *E*, Comparison of day and night Bay K-sensitive currents showing that increasing L-type channel activity activated currents of similar magnitude during both the day and night, thereby eliminating the day versus night difference in current magnitude. *F*, Bay K-sensitive currents normalized to total current, to account for variability in $Ca^{2+}$ current levels between cells. Both day and night currents were increased with Bay K application. However, no significant difference between

day and night current was observed (unpaired *t*-test). N's are the number of neurons recorded (day, night): total $Ca^{2+}$ (96, 82), Nimodipine-sensitive (21, 20), and Bay K-sensitive (9, 9). Data were obtained from 3–8 slices per condition as follows (# slices day, # slices night): Nimodipine-sensitive (8, 8), and Bay K-sensitive (5, 3). *G*, Bay K-sensitive current normalized to the Nimodipine-sensitive current, showing the relative increase for nighttime L-type current is greater than daytime.

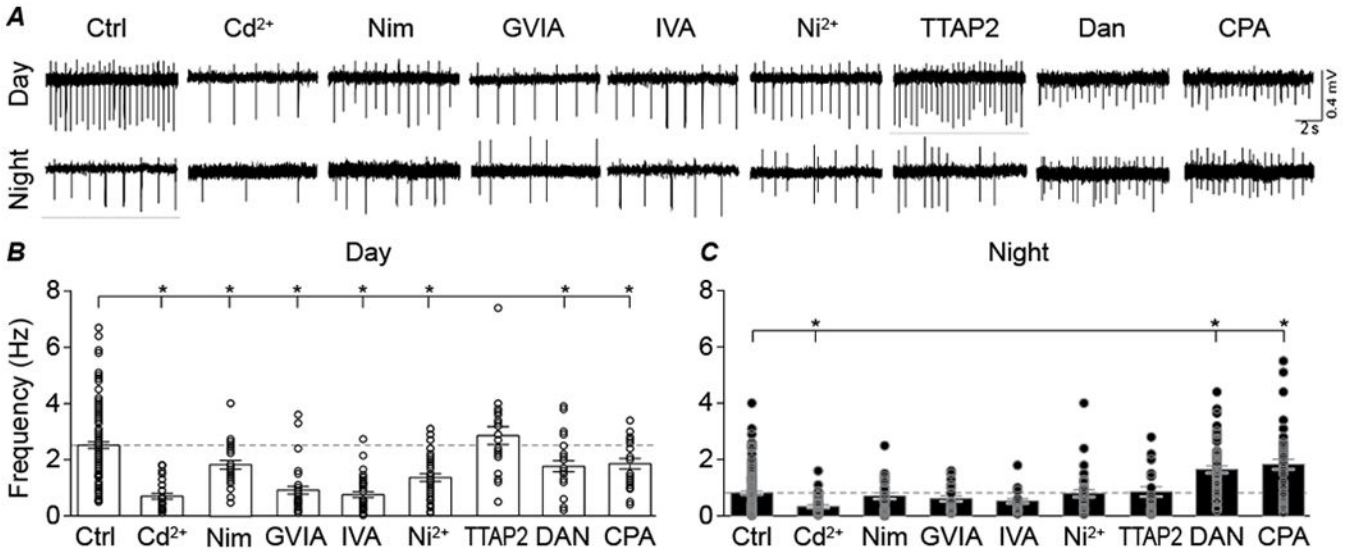


**Figure 7. $Ca^{2+}$ channel inhibitors differentially affect firing frequency of SCN neurons between day and night.**

*A*, Representative extracellular recordings of spontaneous action potential activity recorded from SCN neurons in day and night. *B*, Daytime firing decreased in $Cd^{2+}$ (P=0.01), Nimodipine (P=0.03), ConoGVIA (P=0.01), AgaIVA (P=0.01), $Ni^{2+}$ (P=0.01), Dan (P=0.01) and CPA (P=0.04) compared to control day slices (Ctrl). *C*, Nighttime firing decreased in $Cd^{2+}$ (P=0.01), but increased in Dan (P=0.01) and CPA (P=0.01) compared to control night slices (Ctrl). TTAP2 had no effect on firing in day (P=1) or night (P=1). * P<0.05, One-way ANOVA (Bonferroni correction for multiple comparisons). N's are the number of neurons recorded: Ctrl (n= 119 day, 139 night), $Cd^{2+}$ (n= 26, 35), Nimodipine (n= 27, 31), ConoGVIA (n= 34, 26), AgaIVA (n= 37, 25), $Ni^{2+}$ (n= 38, 34), TTAP2 (n= 20, 21), Dan (n= 25, 55) and CPA (n= 22, 45). Data were derived from 2 slices per condition, except Ctrl (15 day and 16 night slices).

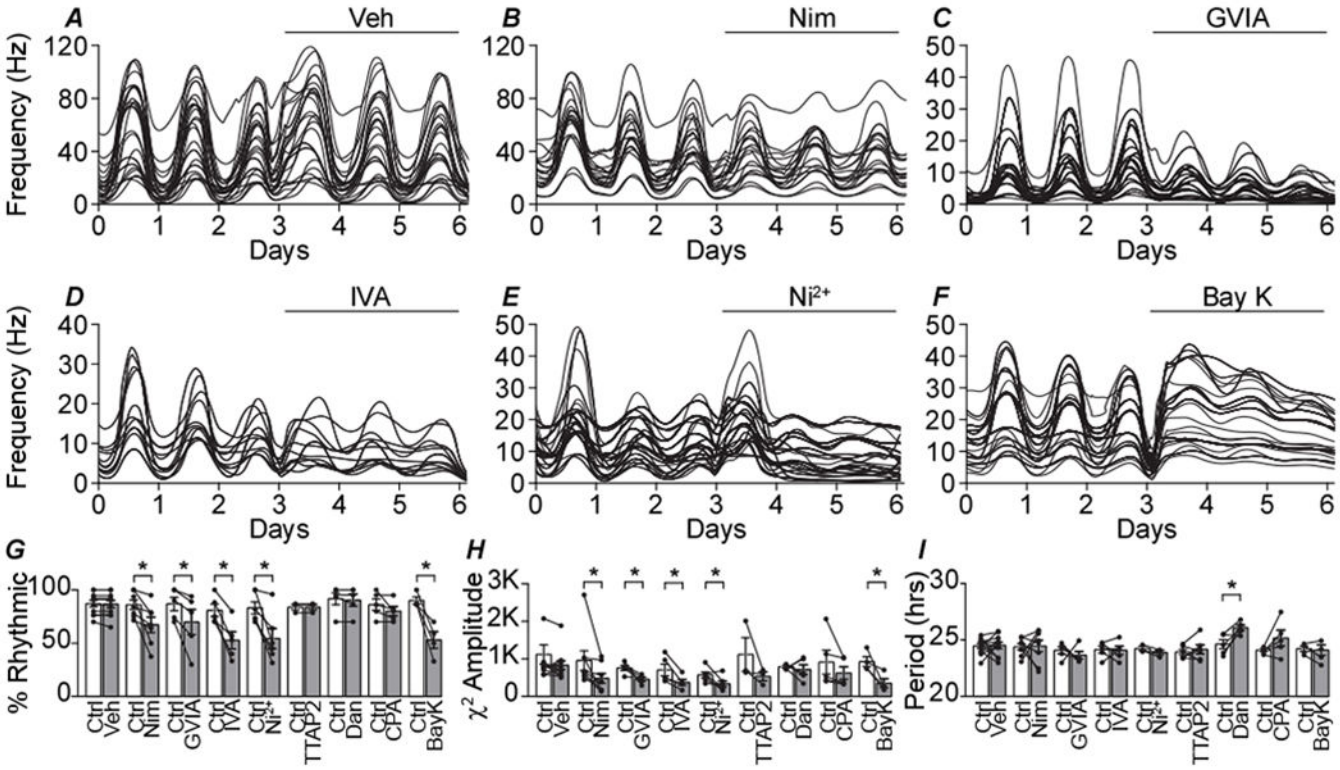


**Figure 8. Effect of $Ca^{2+}$ channel inhibitors on SCN action potential rhythmicity.**

*A-F*, Representative spontaneous action potential activity recorded from organotypic SCN slices over 3 days of baseline control (Ctrl) and 3 days following the application of drugs: vehicle control (Veh) (*A*), 10 μM Nimodipine (*B*), 3 μM ConoGVIA (*C*), 200 nM AgaIVA (*D*), 30 μM $Ni^{2+}$(*E*), 5 μM Bay K (*F*). Each line is firing rate recorded at a single electrode within the SCN. *G*, Percentage of recordings from electrodes within the SCN that exhibited rhythmic firing. Paired *t*-tests were used to compare baseline control to after drug values. The percentage of rhythmic recordings decreased in Nimodipine (P=0.02), ConoGIVA (P=0.04), AgaIVA (P=0.005), $Ni^{2+}$ (P=0.008) and BayK (P=0.02). *H*, $\chi^2$ amplitude quantified from the rhythmic recordings. $\chi^2$ amplitude of rhythmic recordings decreased in Nimodipine, (P=0.04) ConoGIVA (P=0.04), AgaIVA (P=0.03), $Ni^{2+}$ (P=0.04) and BayK (P=0.04). *I*, Period length from the rhythmic recordings. Period length was increased in Dan (P=0.04). Individual data points in panels *G-I* are the slice mean ± SEM values (from the recordings within one slice): Veh (n=198 recordings, 11 slices), Nimodipine (n=123, 8), ConoGVIA (n=91, 5), AgaIVA (n=63, 5), $Ni^{2+}$ (n=84, 5), TTAP2 (n=57, 3), Dan (n=101, 5), CPA (n=93, 5) and BayK (n=75, 4).